Evaluation of Kinetic Models for Industrial Acetic Fermentation: Proposal of a New Model Optimized by Genetic Algorithms

José M. González-Sáiz,*,† Consuelo Pizarro,‡ and Diego Garrido-Vidal†

Chemical Engineering and Analytical Chemistry, Department of Chemistry, University of La Rioja, C/Madre de Dios 51, 26006 Logroño, La Rioja, Spain

The most important kinetic models developed for acetic fermentation were evaluated to study their ability to explain the behavior of the industrial process of acetification. Each model was introduced into a simulation environment capable of replicating the conditions of the industrial plant. In this paper, it is proven that these models are not suitable to predict the evolution of the industrial fermentation by the comparison of the simulation results with an average sequence calculated from the industrial data. Therefore, a new kinetic model for the industrial acetic fermentation was developed. The kinetic parameters of the model were optimized by a specifically designed genetic algorithm. Only the representative sequence of industrial concentrations of acetic acid was required. The main novelty of the algorithm is the four-composed desirability function that works properly as the response to maximize. The new model developed is capable of explaining the behavior of the industrial process. The predictive ability of the model has been compared with that of the other models studied.

Introduction

The main goal in the optimization and automatic control of a bioprocess, such as the acetic fermentation, is large-scale production. Working with a predictive simulation environment is an invaluable tool to develop a bioprocess. The advantages of the process simulation have been performed for a long time now (Cooney et al., 1988; Petrides, 1994), and it is possible to find recent examples of applications of modeling and simulation to the performance and optimization (Cooney et al., 1999; Crundwell, 2001) and predictive control (Hodge and Karim, 2002) of a bioprocess. The basic section in the simulation environment is the process model. This model must be simple in order to explain the whole process with a high predictive ability.

Any bioprocess model has two main parts. One is the reactor model, built with known and very common reactor equations and mass balances, easily found in general books on chemical engineering and bioengineering, such as Perry and Green (1997) and Bailey and Ollis (1986). The other one is the cell growth model and the relationship with the kinetic of substrates and products (Bailey and Ollis, 1986).

In this paper, six kinetic models for acetic fermentation taken from the literature, developed by Bar et al. (1987), Ito et al. (1991), Kruppa and Vortmeyer (1999), Nanba et al. (1984), Park et al. (1991), and Romero et al. (1994), are studied. The kinetic expressions are integrated into a computer environment designed to simulate the behavior of a batch process working with the temperature and oxygen conditions of the industrial process. Comparing the simulation results with an average sequence of acetic acid concentrations calculated from fermentators in the industrial plant of the most important vinegar company in Spain, VINAGRERíAS RIOJANAS S.A., is the method used to test the prediction ability of the models evaluated.

The next step in this work involves the proposal of a new kinetic model specifically designed for the industrial process and the optimization of the kinetic parameters by a genetic algorithm developed for this goal. Genetic algorithms are tools with high potential of optimization that have been successfully applied to solve different problems since Holland published his first works in 1975. Massart et al. (1997) divided the scope of applications of genetic algorithms into three main categories: numerical problems (Reijmers et al., 1999), sequencing problems (Huang, 1997), and subset selection problems (Pizarro et al., 1998). Several tutorials have also been published, such as those by Lucasius and Kateman (1993, 1994) and Wehrens and Buydens (1998).

It is also possible to find works where genetic algorithms have been successfully applied to the empirical modeling of fermentation processes (Potocnik and Grabec, 1999). In this work, the genetic algorithm is developed to optimize the parameters of the new mechanistic model proposed for the industrial acetification. The basic algorithm (Lucasius and Kateman, 1993; Lucasius and Kateman, 1994) has been adapted to this particular problem. The set of kinetic parameters that provide the best prediction ability for the model proposed is selected by the compliance of the simulation with the average sequence obtained from industrial fermentators. One of the most relevant innovations introduced by the algorithm is the desirability function that works successfully as the evaluation function.

Modeling Aspects: Kinetic Models Evaluated

Mechanistic Models: Models with Two Kinds of Biomass. (*A*) *Cell Growth Kinetic.* Some approximations are usually applied to the fermentation models (Bailey and Ollis, 1986). These approximations are very

* To whom correspondence should be addressed. Phone: 0034-941299634. Fax: 0034941299621. E-mail: josemaria.gonzalez@dq.unirioja.es.

† Chemical Engineering.

‡ Analytical Chemistry.

10.1021/bp0256871 CCC: $25.00
Published on Web 02/01/2003

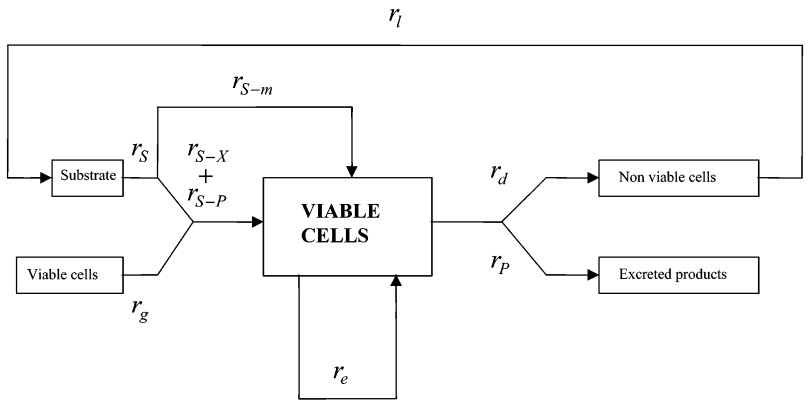

Figure 1. Sinclair's general model for fermentation processes.

necessary and have been used for a long time to obtain simple and predictive models:

• *Average cell approximation*: The cell-to-cell heterogeneity does not influence the model, and the average cellular properties are considered. The model is unsegregated.

• *Balance growth approximation*: The representation of the cell is a single component, and the biomass is considered as a component in solution, X_t. From this point of view, the model is unstructured.

Figure 1 shows the diagram for the reaction mechanisms in fermentation processes proposed by Sinclair and Kristiansen (1987) that is usually assumed. The symbols are reported in the Notation section. The general scheme shows the bacteria divided into viable and nonviable. The viable cells grow with rate r_g and consume the substrate with overall rate r_S. The substrate is used for growing, $r_{S-X,}$ maintenance, r_{S-m}, and product formation, r_{S-P}. As a result of this process, the cells excrete products with rate r_P. On the other hand, the viable cells have a vital cycle and pass to nonviable cells with death rate r_d. The cell death kinetic and the kinetic of products are explained in subsections (B) and (C), respectively. Other mechanisms reported in Figure 1 are the cell lysis, r_l, and the endogenous respiration, r_e. By cell lysis, the nonviable cells are descomposed, and some compounds excreted can be used by the viable cells as substrates. By endogeneous respiration, the cell provides itself the energy for maintenance by the oxidation or degradation of some of the cell mass itself.

In the models proposed by Nanba et al. (1984), Romero et al. (1994), and Bar et al. (1986) and in the model developed in this work, the bacterial mass is considered to be made up of viable X_v and dead X_d cells (Sinclair and Topiwala, 1970). Considering the mechanisms in Figure 1 related only to the cell growth and underestimating the contributions due to cell lysis and endogeneous respiration, the next expressions are inferred, as are applied in the work of Romero et al. (1994), for example:

$$X_v \xrightarrow{r_g} X_v \xrightarrow{r_d} X_d \tag{1}$$

$$X_t = X_v + X_d \tag{2}$$

$$r_g = \frac{dX_t}{dt} \tag{3}$$

$$r_d = \frac{dX_d}{dt} \tag{4}$$

$$r = r_g - r_d = \frac{dX_v}{dt} \tag{5}$$

The specific rates are defined by the overall rates and the viable biomass concentration:

$$\mu_g = \frac{1}{X_v}\cdot\left(\frac{dX_t}{dt}\right) \tag{6}$$

$$\mu_d = \frac{1}{X_v}\cdot\left(\frac{dX_d}{dt}\right) \tag{7}$$

$$\mu = \frac{1}{X_v}\cdot\frac{dX_v}{dt} \tag{8}$$

$$\mu = \mu_g - \mu_d \tag{9}$$

Nanba et al. (1984) proposed the following expression for the overall specific growth rate showing synergistic effects between the ethanol and acetic acid concentrations:

$$\mu_g = \mu_m\cdot\left(\frac{1}{1+\left(\frac{E}{K_i}\right)^4}\right)\cdot\left(\frac{1+\alpha_1\cdot A}{\beta_0+\beta_1\cdot A+\beta_2\cdot A^2+\beta_3\cdot A^3}\right) \tag{10}$$

where:

$$\alpha_1 = K_1 + K_2\cdot E - K_3\cdot E^2 \tag{11}$$

$$\beta_0 = 1 \tag{12}$$

$$\beta_1 = 0 \tag{13}$$

$$\beta_2 = 0 \tag{14}$$

$$\beta_3 = K'_1 + K'_2\cdot E - K'_3\cdot E^2 \tag{15}$$

The experimental data for the parameters fitting were obtained at 28 °C from fermentations in a steady state with different combinations of ethanol [5−75 g/L] and acetic acid [0−50 g/L] concentration prepared with a synthetic medium under nonlimiting oxygen conditions. The calculated values of the parameters are reported in Table 1. The kinetic parameter K_i is the inhibition constant related to the ethanol concentration. The other parameters reflect the synergistic effects between the ethanol and the acetic acid.

Bar et al. (1987) proposed an empiric expression for the specific growth rate that shows a strong cell inhibition by the acetic acid:

Table 1. Kinetic Parameters of the Models Evaluated

model									
Nanba et al.		Romero et al.		Park et al.		Ito et al.		Kruppa and Vortmeyer	
parameter	value	parameter	value	parameter	value	parameter	value	parameter	value
μ_m	0.31 h^{-1}	μ_m	0.22 ± 0.02 h^{-1}	μ_m	0.25 h^{-1}	c	3.5 × 10^{-5}	μ_m	0.1565 h^{-1}
K_i	91 g/L	$\mu_m^{29.°C}$	0.088 h^{-1}	A_m	45 g/L	$n = m$	2	C_μ	105.9 g/L
K_1	7.170 × 10^{-2}	K_{SE}	21.1 ± 6.7 g/L	$n = m$	1.766	q_{Am}	20 h^{-1}	r_m	0.35 mol/(g·h)
K_2	2.228 × 10^{-3}	K_{IE}	2.83 ± 0.2 g/L	μ_{cm}	0.05 h^{-1}	A_{qm}	90 g/L	C_r	93.8 g/L
K_3	2.822 × 10^{-5}	K_{SA}	12.6 ± 2.5 g/L	$A_{cm} = A_{qm}$	95.1 g/L	γ	0.03 h^{-1}	a_r	0.0219 mol·L/(g^2·h)
K'_1	1.0480 × 10^{-4}	K_{IA}	17.9 ± 1.2 g/L	a	0.2 h^{-1}			b_r	0.060 mol/(g·h)
K'_2	7.041 × 10^{-6}	K_{SO}	0.372 ± 0.05 ppm	b	0.037				
K'_3	7.873 × 10^{-8}	K_{IO}	1.958 ± 0.21 ppm	q_{Am}	33.3 h^{-1}				
		A	0.5 h^{-1}						
		B	8.97 × 10^{-7} h^{-1}						
		E_b	5.974 kJ/mol						
		E_a	417.2 J/mol						
		K_m	0.42 L/g·h						
		K_N	2.50 × 10^7 $(g/L)^3$						

$$\mu_g = 0.119 \times e^{(-0.068 \cdot A)} \tag{16}$$

The data were taken from fermentators thermostated at 30 °C under low aeration conditions. No more than 36.5 g/L of acetic acid were obtained with a synthetic medium.

Romero et al. (1994) proposed an expression that takes into account the ethanol, acetic acid, and oxygen concentrations:

$$\mu_g = \mu_m \cdot \left(\frac{E}{E + K_{SE} + \left(\frac{E}{K_{IE}}\right)^2}\right) \cdot \left(\frac{1 + \left(\frac{A}{K_{SA}}\right)}{1 + \left(\frac{A}{K_{IA}}\right)^3}\right) \cdot \left(\frac{\left(\frac{O}{K_{SO}}\right)}{1 + \left(\frac{O}{K_{IO}}\right)^3}\right) \tag{17}$$

In this expression, there are two kind of parameters. Parameters as K_{SE}, K_{SA}, and K_{SO} correspond to saturation constants for ethanol, acetic acid, and oxygen, respectively, and reflect the metabolic affinity of the microorganism for them. Parameters as K_{IE}, K_{IA}, and K_{IO} are the inhibitory parameters for ethanol, acetic acid, and oxygen, respectively, and quantify the inhibiting effect of these compounds over the specific growth rate. High values of the saturation constant reflect a low microorganism-compound affinity, whereas high values of the inhibition constant reflect a low level of substrate inhibition.

The data were obtained in batch fermentations at 26 °C, and the concentration ranges studied were 10−70 g/L for ethanol and 10−80 g/L for acetic acid, using as medium sterilized wine from the region of Jerez.

In a subsequent work, Ory et al. (1998) calculated the parameters of the expression proposed by Sinclair and Topiwala (1970) for μ_m, using eq 17 to obtain the values of μ_m:

$$\mu_m = A \cdot e^{-E_a/RT} - B \cdot e^{-E_b/RT} \tag{18}$$

The values for the kinetic parameters of eqs 17 and 18 are reported in Table 1.

(B) Cell Death Kinetic. Generally, the kinetics of growth and death are modeled separately because of the different effects of the variables in each case. In their work, Mesa et al. (1994) proposed the following expression for the specific death rate under conditions of complete absence of oxygen:

$$\mu_d = \frac{K_M \cdot A^4}{E^3 + K_N} \tag{19}$$

The values for the parameters were $K_M = 0.11$ L/g·h and $K_N = 3.54 \times 10^3$ $(g/L)^3$. Later, Caro et al. (1996) recalculated the values to apply the expression under nonanoxic conditions: $K_M = 0.42$ L/g·h and $K_N = 2.50 \times 10^7$ $(g/L)^3$.

(C) Substrates and Products Kinetic. Applying Sinclair's general model to the substrates and the products, the following expressions are obtained:

$$r_E = r_{E-x} + r_{E-m} + r_{E-P} + r_{E-AcEt} \tag{20}$$

$$r_O = r_{O-X} + r_{O-m} + r_{O-P} \tag{21}$$

$$r_A = r_{A-X} - r_{A-AcEt} \tag{22}$$

It is reasonable to consider that, in acetic fermentation, the energy requirements of the cells are basically due to the multiplication process, and thus other consumptions are worthless and the mean contribution is the assimilative way. The lacks due to ethyl acetate production are not significant since they account for less than 3% of the total ethanol consumption. Therefore, these expressions can be simplified:

$$r_E = r_{E-x} \tag{23}$$

$$r_O = r_{O-X} \tag{24}$$

$$r_A = r_{A-X} \tag{25}$$

It is very usual to link the product formation and the substrate consumption with the cell growth. These substrates and products kinetics are usually called growth-associated (Bailey and Ollis, 1986):

$$\frac{dE}{dt} = \left(-\frac{1}{Y'_{X/E}}\right) \cdot \mu_g \cdot X_v \tag{26}$$

$$\frac{dO}{dt} = \left(-\frac{1}{Y'_{X/O}}\right) \cdot \mu_g \cdot X_v \tag{27}$$

$$\frac{dA}{dt} = Y_{A/E} \cdot \frac{1}{Y'_{X/E}} \mu_g \cdot X_v \tag{28}$$

The most important yield factor is $Y'_{X/E}$. Different values for the biomass/ethanol yield factor can be found

in the literature, depending mainly on the operation conditions and the ethanol losses by evaporation.

In their work, Bar et al. (1987) established a growth-associated acetic acid kinetic and a stoichiometric relationship between ethanol and acetic acid. On the basis of Romero et al.'s growth model (1994), Gómez and Cantero (1998) proposed a growth-associated model for the kinetics of ethanol, oxygen, and acetic acid:

$$Y'_{X/E} = (7.2 \pm 0.8) \times 10^{-3} \text{ g biomass/g ethanol}$$

(Gómez and Cantero, 1998)

$$Y'_{X/E} = 6 \times 10^{-3} \text{ g biomass/g ethanol}$$

(Bar et al., 1987)

The values of the stoichiometric coefficients $Y_{A/E}$ and $Y_{E/O}$ are 1.30 and 1.44, respectively, and the biomass/oxygen yield factor can be easily calculated:

$$Y'_{X/O} = Y_{E/O} \cdot Y'_{X/E} \tag{29}$$

Mechanistic Models: Models with Three Kinds of Biomass. Ito et al. (1991) and Park et al. (1991) proposed more complex kinetic models from a mechanistic point of view, with three classes of biomass: viable, nonviable, and dead and without a relationship between the cell growth and the kinetics of the substrates and the product. The general scheme of these two models is:

$$X_v \xrightarrow{\mu_g} X_v \xrightarrow{k} X_{nv} \xrightarrow{\gamma} X_d \tag{30}$$

$$E \xrightarrow{q_A \cdot (X_v + X_{nv})} A \tag{31}$$

$$O \xrightarrow{q_A/Y_{A/O},\ \mu/Y'_{X/O}} X_v,\ A \tag{32}$$

Taking into account eq 30, viable cells are converted via nonviable cells into dead cells when the acetic acid concentration is higher than a critical concentration, which will depend on the kinetic parameters calculated for the specific growth rates μ, k, and γ, but the ethanol and the oxygen are not depleted. Both viable and nonviable cells can oxidize the ethanol, but nonviable cells cannot multiply. In this way, in eq 31, the rate of ethanol consuming depends on the specific rate q_A and on the concentrations of viable and nonviable biomass, X_v and X_{nv}, respectively. In eq 32 is shown that, in this model, oxygen is consumed not only to oxidize the ethanol to acetic acid ($q_A/Y_{A/O}$) but also for the cell respiration ($\mu/Y'_{X/O}$).

From this pattern, the following differential equations are inferred:

$$\frac{dX_v}{dt} = (\mu_g - k) \cdot X_v = \mu \cdot X_v \tag{33}$$

$$\frac{dX_{nv}}{dt} = k \cdot X_v - \gamma \cdot X_{nv} \tag{34}$$

$$\frac{d(X_v + X_{nv} + X_d)}{dt} = \mu_g \cdot X_v \tag{35}$$

$$\frac{dX_d}{dt} = \gamma \cdot X_{nv} \tag{36}$$

$$\frac{dA}{dt} = q_A \cdot (X_v + X_{nv}) \tag{37}$$

$$\frac{dE}{dt} = -\frac{1}{Y_{A/E}} \cdot q_A \cdot (X_v + X_{nv}) \tag{38}$$

$$\frac{dO}{dt} = \left(-\frac{1}{Y_{A/O}} \cdot \frac{dA}{dt}\right) + \left(-\frac{1}{Y'_{X/O}} \cdot \frac{dX_v}{dt}\right) \tag{39}$$

In their work, Park et al. (1991) proposed the following expressions for the specific rates:

$$\mu = \mu_g - k = \mu_m \cdot \left[1 - \left(\frac{A}{A_m}\right)^n\right] \tag{40}$$

$$\mu_g = \mu_{cm} \cdot \left(1 - \frac{A}{A_{cm}}\right) \tag{41}$$

$$k = \mu_g - \mu = \mu_{cm} \cdot \left(1 - \frac{A}{A_{cm}}\right) - \mu_m \cdot \left[1 - \left(\frac{A}{A_m}\right)^n\right] \tag{42}$$

$$\gamma = a \cdot e^{(b \cdot A)} \tag{43}$$

$$q_A = q_{Am} \cdot \left[1 - \left(\frac{A}{A_{qm}}\right)^m\right] \tag{44}$$

In these equations, kinetic parameters A_m, A_{cm}, and A_{qm} are inhibition parameters related to the acetic acid concentrations in the specific growth rates μ and μ_g and the acetic growth rate q_{Am}, respectively. A_{cm} in eq 41 and A_{qm} in eq 44 mean the maximum concentration at which all the biological activities of the cells are lost. The constants n and m are experimental exponents and indicative of how strongly the inhibition terms affect μ and q_A, respectively. The parameters a and $b$are experimental constants which express the effect of acetic acid on cell death.

The data were obtained from a batch fermentator thermostated at 30 °C, under no-limiting oxygen conditions in a synthetic medium. The concentration of ethanol was kept between 20 and 30 g/L by a feed flow of 500 g/L ethanol. The maximum concentration of acetic that this system could reach was 85 g/L. Table 1 reports the values calculated by Park et al. for the kinetic parameters.

One of the main obstacles of the model is that viable and nonviable biomass are considered to have the same energy requirements, whereas nonviable biomass is unable to multiply. Another is caused by the negative values taken by the specific rate k when the concentration of acetic acid is under 10 g/L.

Ito et al. (1991) developed a model based on Park et al.'s model but introducing some changes in the specific rates μ_g, k, and γ. The main innovation is that they take the expression of Nanba et al.'s model for μ_g with the same values for the kinetic parameters:

$$\mu_c = \mu_{max} \cdot \frac{1}{1 + \left(\frac{E}{K_i}\right)^4} \cdot \left(\frac{1 + \alpha_1 \cdot A}{\beta_0 + \beta_1 \cdot A + \beta_2 \cdot A^2 + \beta_3 \cdot A^3}\right) \tag{45}$$

$$\mu = \mu_c - k \tag{46}$$

$$k = c \cdot A^n \tag{47}$$

$$q_A = q_{Am} \cdot \left[1 - \left(\frac{A}{A_{qm}}\right)^m\right] \tag{48}$$

The experimental data were obtained in a fermentator working under conditions similar to those of Park et al.'s,

but with a constant ethanol concentration of 10 g/L. The maximum acetic acid concentration reached was 90 g/L. The values calculated for the parameters are reported in Table 1.

The model solves the problems of Park et al.'s model, but more empiric expressions without mechanistic significant are introduced.

Empiric Model: Kruppa and Vortmeyer's Model. In their work, Kruppa and Vortmeyer (1999) proposed an empirical model for the rates of cell growth and acetic acid production without any relationship between them, i.e., they did not establish any relationship between the cell growth and the kinetics of the substrates and the product:

$$r_g = \mu_m \cdot \left(1 - \frac{A}{C_\mu}\right) \cdot X_t \tag{49}$$

$$r_E = M_{EtOH} \cdot \left[r_m - \frac{1}{2} \cdot ((a_r^2 \cdot (A - C_r)^2 + b_r^2)^{1/2} + a_r \cdot (A - C_r))\right] \cdot X_t \tag{50}$$

$$r_A = M_{HAc} \cdot \left[r_m - \frac{1}{2} \cdot ((a_r^2 \cdot (A - C_r)^2 + b_r^2)^{1/2} + a_r \cdot (A - C_r))\right] \cdot X_t \tag{51}$$

As a result of the empirical nature of the model, there is no classification of biomass in terms of viability. Table 1 reports the values of the kinetic parameters calculated in the work. The data were obtained from a continuous fermentator, thermostated at 30 °C and under nonlimiting oxygen conditions; therefore there is no expression for the oxygen. In each steady state an acetic concentration within the range of 50−100 g/L and the corresponding concentration of ethanol were obtained, taking into account that the feed flow was an artificial medium with concentrations of 77.3 g/L for ethanol and 1 g/L for acetic acid.

New Model for Industrial Acetification

Analysis of Industrial Data Set. The acetic concentrations taken from the industrial fermentators in the industrial plant, obtained by near-infrared spectroscopy, NIR, (Osborne et al., 1993) were studied. The data were collected for four months without changes in the industrial parameters of the process, i.e., oxygenation conditions and temperature. The average temperature was 29.5 °C and the oxygenation conditions were enough to satisfy the oxygen demand, and thus the oxygen was a nonlimiting substrate. The total biomass was measured by filtration, drying, and weighing of the sample.

Nowadays, fermentators in the industrial plant work discontinuously with charges. The batch bioreactors studied were always fed with white wine of the same origin. The process time was about 30−31 h, and 218 complete sequences were obtained.

An average concentration sequence was calculated by analyzing the data. This sequence is representative of the process to be modeled. The variability in the concentrations among the sequences is due to analytical errors and to factors that cannot be controlled in an industrial process, i.e., differences in ethanol concentration of wine among the batch processes. Therefore, the model obtained with this sequence does not model this variance. Figure 2 shows the average concentrations sequence.

Structure of the New Kinetic Model. The model proposed assumes the general pattern of Sinclair and Kristiansen (1987) reported in Figure 1 for the cell growth, despising the contributions due to cell lysis and endogeneous respiration. The average cell and the balance growth approximations are applied to the cell model, i.e., the model developed is unsegregated and unstructured:

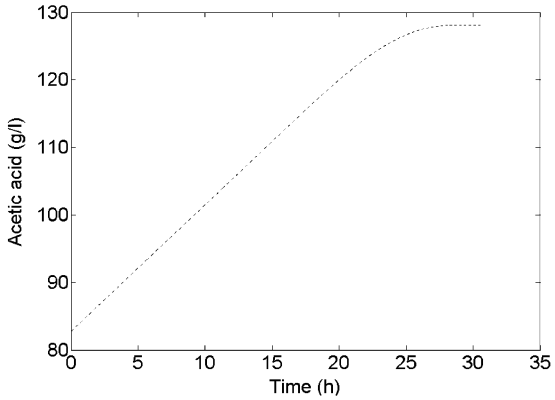

Figure 2. Representative data sequence calculated from the industrial concentrations.

$$X_v \xrightarrow{r_g} X_v \xrightarrow{r_d} X_d \tag{52}$$

$$X_t = X_v + X_d \tag{53}$$

$$r_g = \frac{dX_t}{dt} \tag{54}$$

$$r_d = \frac{dX_d}{dt} \tag{55}$$

$$r = r_g - r_d = \frac{dX_v}{dt} \tag{56}$$

The specific rates are defined by the overall rates and the viable biomass concentration, as has been explained before:

$$\mu_g = \frac{1}{X_v} \cdot \left(\frac{dX_t}{dt}\right) \tag{57}$$

$$\mu_d = \frac{1}{X_v} \cdot \left(\frac{dX_d}{dt}\right) \tag{58}$$

$$\mu = \frac{1}{X_v} \cdot \frac{dX_v}{dt} \tag{59}$$

$$\mu = \mu_g - \mu_d \tag{60}$$

A growth-associated kinetic for the acetic acid production and the oxygen and ethanol consumption is proposed, according to the pattern of substrates and products kinetic reported for the models studied in the section **Mechanistic Models: Models with Two Kinds of Biomass**:

$$\frac{dE}{dt} = \left(-\frac{1}{Y'_{X/E}}\right) \cdot \mu_g \cdot X_v \tag{61}$$

$$\frac{dO}{dt} = \left(-\frac{1}{Y'_{X/O}}\right) \cdot \mu_g \cdot X_v \tag{62}$$

$$\frac{dA}{dt} = Y_{A/E} \cdot \frac{1}{Y'_{X/E}} \mu_g \cdot X_v \tag{63}$$

The main statement of the model proposed is based on the fact that the viable cells oxidize the ethanol to acetic acid to obtain the energy that they need for multiplication. The structure of the model is based on the existence of two kinds of biomass as in the models of Bar et al. (1987), Nanba et al. (1984), and Romero et al. (1994). The existence of a third class of biomass, proposed in the models of Park et al. (1991) and Ito et al. (1991) is only theoretical, since there are no measures of this kind of biomass. The supposed behavior of the nonviable cells is not justified considering the fact that the nonviable biomass is not capable of multiplying but it is considered to have the same energy requirements of the viable cells. On the other hand, Park et al.'s model has another important drawback due to the existence of nonviable cells, considering the negative values taken by the specific rate k in eq 42 when the concentration of acetic acid is under 10 g/L. The work of Ito et al. (1991) corrected these wrong estimations by introducing in the model new empirical equations without mechanistic fundament.

All in all, the introduction of the third class of biomass adds a grade complexity to the models without an improvement on the explanation of the acetic fermentation, compared with the models with two kinds of biomass.

Assuming that the industrial data show a decrease in the acetic production only due to the ethanol consumption, a function for μ_g based exclusively on the ethanol concentration is proposed, because no inhibition due to acetic acid is observed in the industry. Indeed, in fermentation processes with alcoholic substrates of agricultural origin are obtained acetic concentrations of about 150 g/L and less than 4 g/L for the residual ethanol. There is no oxygen concentration factor since in the industrial fermentation processes the oxygen demand is always satisfied by a constant aeration and agitation, and thus oxygen is a nonlimiting condition:

$$\mu_g = K_1 \cdot \frac{1}{K_2 + \left(\frac{1}{E}\right)^n} \tag{64}$$

In this model, μ_d is considered to be constant, since it is logical to evaluate an average life cycle from the average cell approximation applied to the model.

The initial viable biomass, X_{vi}, influences very much the rate of the process. No measures of biomass viability were available in the industrial plant, and thus the initial concentration must be optimized together with the kinetic parameters. In this model with two kinds of biomass, the initial total biomass does not influence the evolution of the fermentation, and therefore it takes the value of the initial viable biomass in the optimization algorithm. In this way, the initial viable biomass is not constrained by the value of the total biomass and can take any value within the range externally imposed.

All in all, the problem to be solved was the optimization of five parameters of the model: K_1, K_2, n, μ_d, and X_{vi}.

Computational Methods

Simulation Method. The simulation algorithm was programmed in Matlab 6.1.0.450 (The MathWorks, Inc.). The critical points of the algorithm were

(1) The kinetic model: a differential equations system solved by the fourth order Runge−Kutta algorithm.

(2) The kinetic parameters: the parameters calculated by the authors in the original works were used.

(3) The mass balance for the fermentator: a batch process was simulated.

(4) The fermentator parameters: (a) the volume was constant: 30 000 L; (b) there was an oxygen control in the simulation, because in the industrial process the oxygenation conditions were enough to satisfy the oxygen demand.

(5) Initial values of the variables: the initial concentrations of ethanol, acetic acid, and total biomass were those of the representative sequence, 40.14 g/L of ethanol, 82.73 g/L of acetic acid, and 0.35 g/L of total biomass. No measures of initial viable biomass were available in the industry. Therefore, it was considered to be 20% over the initial total biomass, a standard value used in other works of computer simulation of fermentation processes, such as Caro et al. (1996) and Macías et al. (1997) for a started fermentation.

(6) Evaporation losses of ethanol and acetic acid were not considered. In this way, the simulated reactor was a closed system.

(7) The simulation algorithm had two important stoppage conditions: (a) the simulation was stopped when not real positive values for one concentration were obtained; (b) the simulation was stopped when the process time in the simulation reached the final process time of the representative sequence.

Genetic Algorithms Applied to Kinetic Modeling. Genetic algorithms are numerical optimization methods that try to simulate the biological evolution, i.e., the process of optimization of the characteristics of the individuals to improve their adjustment to the environment. Those that adjust the best to the environment have more chances of surviving and reproducing.

Applied to biological modeling, the use of genetic algorithms implies many advantages over the use of the traditional gradient-search and graphical methods. Those methods often provide solutions at local minima and convergence problems have been noted when gradient-based methods have been applied to biological models (Pinchuk et al., 1999). The genetic algorithm optimization does not rely on the mathematical form of the kinetic model, simplifying the optimization process and allowing test different models without modifying the algorithm. Other classic methods of optimization exist that do not use the gradient of the objective function, like the Simplex or the Powell methods. The main disadvantages of these methods are that they need a starting point, they do not work well with badly behaved statistic surfaces, and there is no guarantee they will find the global optimum, a problem long known specially with the Simplex method. The Simplex has also important convergence problems. The genetic algorithm allows a better exploration of the experimental domain, avoiding convergence to a relative optimum due mainly to

(1) An initial estimate of the parameters is not required, but rather a range of possible values. With Simplex or Powell method the solution depends heavily on the chosen starting point.

(2) The mutation operator allows the algorithm to escape from an area of chromosomes closed to a local maximum to another areas in the allowed range, preventing the premature convergence to a suboptimal solution.

(3) The crossover operator allows the exchange of information between promising solutions. The use of the uniform crossover instead of the crossover points limited to locations between genes increases the genetic diversity of the offsprings and the exploration of new areas of the domain.

Table 2. Description of Genetic Algorithm

parameter	description
coding	Binary. Each chromosome is a different set of the kinetic parameters to optimize. The number of bits of the chromosome depends on the range allowed for the parameters and the amount of significant figures, fixed previously.
initiation of population	Random. Out-of-range chromosomes are not generated.
population	30 chromosomes. The population is constant.
response	Four-composed desirability function.
select-copy	The probability of a chromosome of being selected for crossover is $prob(i) = (response(i)/sum(responses))$. An interval of random number is associated to each genome, with upper limit the cumulative sum of probabilities of the chromosomes with inferior probability of being selected. Then, the algorithm generates random numbers (0−1). When the number is within the interval associated to a chromosome, this is selected for crossover.
crossover	Uniform crossover. Crossover probability 50%.
mutation	1.5%
elitism	The six best chromosomes of each generation pass unchanged to the following generation.
filters	Out-of-range parameters and twins are not allowed.
stoppage condition	Five generations without changes higher than 5% in the mean response of the elitist chromosomes.
heats and final	The algorithm is completed five times each time the programmed algorithm is run. A final run where the initial population is composed of the best chromosomes found in each of the previous runs is performed.
software	Matlab 6.1.0.450. (The MathWorks, Inc.).

(4) The solution provided by the genetic algorithm is not unique; a series of almost equivalent results is obtained and the user can select the best.

All in all, the use of genetic algorithms allows finding the optimized parameters even for poorly behaved functions. At every moment, every point of the experimental domain can be explored.

The algorithm designed in this work is an evolution of the basic genetic algorithm (Lucasius and Kateman, 1993; Lucasius and Kateman, 1994), adapted to find the best set of parameters for the new kinetic model proposed. Each chromosome represents a possible combination of values of the five parameters to optimize, in binary code. There is an allowed range of values for each parameter to adopt as many values as allowed by the binary codification and the amount of significant figures. The evaluation program decodes the values of the parameters for each chromosome and then uses them to simulate a batch process with each set of parameters. Uniform crossover and mutation operators are used to form new generations of chromosomes. The elitism, i.e., a number of chromosomes that passed unchanged to the following generation, is introduced to avoid the loss of highly informative solutions. Filters are introduced into the algorithm to avoid twins and out-of-range parameters. A final run with the best chromosomes found in several runs is made as refinement of the best solutions found and, therefore, to increase the exploitation ability of the method. In conclusion, the uniform crossover, the mutation, the elitism, the filters, and the final run contribute to the exploration and the exploitation ability of the algorithm.

The same simulation program and conditions as those used with the models evaluated before were applied, but the value for the initial viable biomass was that of the parameters of the chromosome. The main technical features of the algorithm are reported in Table 2.

The most important innovation of the algorithm developed in this work is the desirability function that works as the evaluation function to maximize. The evaluation function of the genetic algorithm must be capable of selecting the best set of kinetic parameters, those that provide the highest predictive ability to the model, obtaining simulated acetic concentration sequences similar to the industrial ones.

The root-mean-square of the differences between measured and predicted data or other similar functions based only on the errors have been extensively used in the performance of artificial neural networks, as the work of Shimizu et al. (1998), or as the evaluation function of the genetic algorithm, as Pinchuk et al. (1999). However, the root-mean-square is not enough in this work to compare the concentration sequences since it does not provide information on the differences in the shape of the data sequence, the final concentration reached, and the process time.

To solve the problem, a four-composed desirability function has been applied as the response to maximize. The desirability functions are one of the methods for Multicriteria Decision Making (MCDM) (Harrington, 1965; Hendriks et al., 1992; Keller et al., 1991; Massart et al., 1997). It is possible to find recent works where desirability functions are used for multiresponse optimization, such as Berget and Naes (2002).

A desirability function has to be defined for each criterion considered. Each function can adopt different mathematical structures such as linear, exponential, or logarithmic ones, but the response must always range between 0 (unacceptable) and 1 (maximum desirability). The global desirability function for the *n* sample is then defined as the geometric mean of the individual desirability functions:

$$d_{cn} = f_c(y_{cn}); \qquad 0 \le d_{cn} \le 1 \tag{65}$$

$$D_n = \left(\prod^{c} d_{cn}\right)^{1/c} \tag{66}$$

The mathematical form of the desirability function developed in this work is

$$R = \left[\underbrace{\left(\frac{1}{1+RMS}\right)}_{1} \cdot \underbrace{\left(\frac{t_s}{t_r}\right)}_{2} \cdot \underbrace{\left(\frac{1}{1+abs\left(A_s - A_r\right)}\right)}_{3} \cdot \underbrace{\left(\frac{1}{1+abs\left(atan\left(B_s\right) - atan\left(B_r\right)\right)}\right)}_{4} \right]^{1/4} \tag{67}$$

The main advantages of working with the desirability function instead of using only the root-mean-square are:

• The global function is very restrictive because if only one single function gives a zero value, the global value is zero. This behavior has been useful to penalise seriously the sets of parameters providing simulations with

concentrations lacking any analytical significance, such as negative values, since they are stopped without reaching the final process time and the final acetic concentration of the representative sequence. With these sequences values close to zero are obtained for the functions 2 and 3 of eq 67, although RMS values are not so bad due to the limited points to compare. The sets of parameters that provide extremely fast simulated processes are also penalized because the final process time is very low compared to the final process time of the representative sequence, so the value of function 2 in eq 67 is close to zero. The sets of parameters providing very slow simulated processes are penalized since the simulation is always stopped when the final process time of the representative sequence is reached, and thus the RMS is very high and the acetic concentration reached is very low, and thus the values of functions 1 and 3 in eq 67 are very low. All in all, the sets of kinetic parameters providing extremely long or short process times in the simulation and/or reaching a final acetic concentration far from the real sequence have been seriously penalized.

• On the other hand, all the single functions must give maximum values to obtain a maximum global value, conferring a more selective power on the evaluation function, particularly in simulated sequences with a similar low value for the RMS and with a final process time and a final acetic acid concentration similar to those of the representative sequence but with very different shapes. In this case, the sets of kinetic parameters providing a sequence data with a linear segment in the simulation similar to the data with a linear behavior in the real data sequence are rewarded, because a value very close to 1 is reached for the function 4 in eq 67.

• The desirability function is scaled between 0 and 1, allowing for an objective comparison of the adjustment of each simulation to the representative sequence.

In short, the desirability function provides better discrimination abilities for the algorithm than the RMS method.

Results and Discussion

Predictive Ability of the Kinetic Models Evaluated. Some specific considerations were applied to the simulations:

• Nanba et al. do not propose any specific relationship between their expression for μ_g and the kinetic for the product and the substrates, but a growth-associated kinetic (eqs 26−28) was assumed to be the most suitable one.

• Nanba et al. and Bar et al. did not model the death rate, and thus the expression proposed by Mesa et al. (1994) was applied with the parameters recalculated by Caro et al. (1996).

• The value for the coefficient $Y'_{X/E}$ was that calculated by Gómez and Cantero (1998), since it provides with a good estimation in a closed system without evaporation losses. The value for $Y'_{X/O}$ was calculated from eq 29, taking a value 1.04×10^{-2}. With Park et al. and Ito et al.'s models, the value calculated by Park, 1.32×10^{-2}, was used.

• The initial nonviable biomass in simulations with Park et al. and Ito et al.'s models was considered to be zero. According to these models, the nonviable biomass appears only when a particular level of acetic acid is reached.

• With Romero et al.'s model, the value of μ_m was calculated with eq 18 to simulate the process at 29.5 °C, the average temperature for industrial fermentation. In the other simulations, the experimental data to adjust the parameters of each model were taken with temperatures very close to 29.5 °C, i.e., 30 and 28 °C (Nanba et al.'s model).

• Oxygen conditions in the simulation with Romero et al.'s model (1994) were controlled to keep the oxygen concentration constant at 1.6 ppm, the optimum value calculated in their work. In the other simulations, the oxygen concentration did not have any impact at the specific rates and therefore the oxygen control kept the concentration constant at 0 ppm, simulating the industrial process, where the oxygen required is contributed to the cell.

• In their work, Park et al. did not provide the value of the kinetic parameter m. For the simulation, it was considered that it takes the same value as n (1.766), as it had been considered in the work by Ito et al.

To sum up, six simulations were developed. The acetic acid concentrations provided by the simulations are reported and compared in Figure 3. It is shown that the simulations stopped between approximately 83 and 100 g/L, depending on the model. The acetification rates were very low in five of the models, less than 0.5 g/(L·h), but with the Kruppa-Vortmeyer model, a high rate was calculated, although the simulation finished with less than 110 g/L of acetic acid. Despite that, with this model the simulation best adjusted to the real sequence was obtained. A high concentration of residual ethanol was unoxidized, according to these models.

The main reason for this bad predictive capability is the inhibition by the acetic acid accumulation proposed in each model. The industrial process does not exhibit such an inhibition; indeed, the fermentation processes of alcoholic substrate different from wine reach acetic concentrations of about 150 g/L. Therefore, the decrease in the rate of acetification can only be related to a decrease in the cell growth due to ethanol consumption.

On the other hand, the data for most of the works were taken in laboratory systems under conditions very different from the real ones in an industrial plant and in highly idealized mediums in most of the cases, when the bacteria are actually able to adjust their life cycle to hard mediums as the industrial ones, without sterilization, nutrients, or ideal pH conditions. Furthermore, in some cases such as the work by Bar et al. (1987), a limitation in the experimental conditions (it was only possible to obtain 40 g/L because of the initial ethanol concentration) makes the model detect a false inhibition of the cell growth with concentrations of acetic acid higher than 40 g/L, when this is actually due to the depletion of ethanol.

To conclude, these models with the original calculation of the kinetic parameters are unable to explain the behavior of the industrial acetification. Therefore, a new kinetic model is required to model the fermentation and to develop a proper simulation tool in order to optimize the process and propose new fermentation systems.

Parameters Optimization of New Model by Genetic Algorithm Developed. The genetic algorithm is stochastic, and thus after running the program several times, an optimized set of parameters was obtained. The ranges allowed for n, μ_d, and X_{vi} were the logical ones from the point of view of the biological knowledge of the model proposed. The ranges for K_1 and K_2 were very large in the first runs to explore the whole experimental domain and find the areas with the best predictive ability. Then, these areas were studied to find the best zone and gradually the allowed range was shortened until the range with which the last runs were performed was obtained.

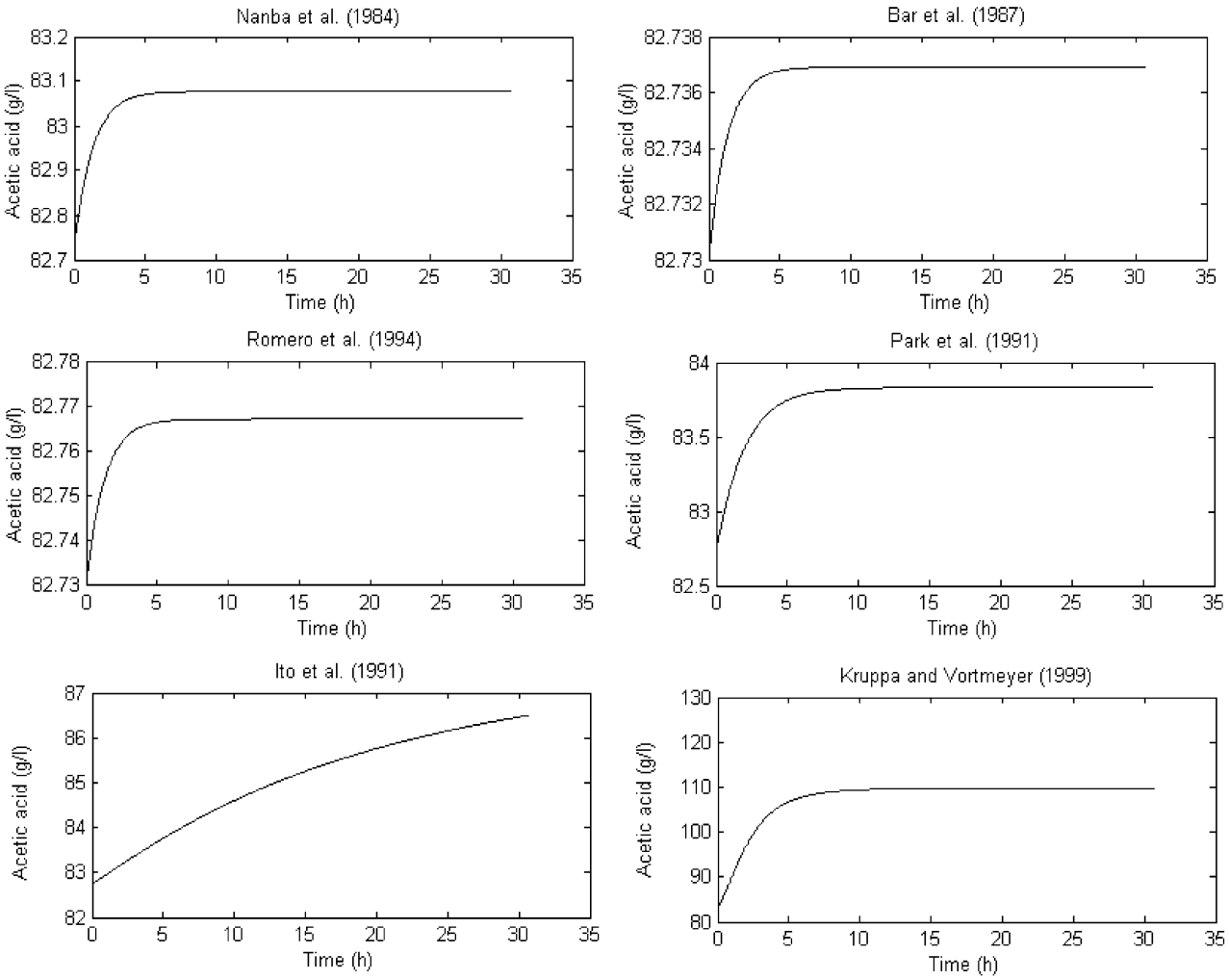

Figure 3. Acetic acid concentrations obtained in simulation with the models evaluated.

This methodology cannot be applied with an ordinary nonlinear regression technique, where an initial estimate of the values of the parameters is required.

The optimized set of parameters is reported in Table 3. Figure 4 shows the output of the simulation for the batch process with the optimized new model. The high ability of the model to simulate the evolution of the concentrations in industrial fermentators is shown in the comparison with the representative sequence of the industrial process (dotted line) and even more in the graphic that represents the predicted acetic acid concentrations versus the measured acetic acid concentrations. A very low value for the RMS is obtained (0.0023), the values of the final process time and the final acetic acid concentration simulated are almost the same as in the representative sequence, and the linear segment of the simulation data is very close to the linear segment of the representative sequence, so a high value for the response of the genetic algorithm, 0.92, is provided.

In Figure 5 the values for the RMS and the response multiplied by a factor of 1000 obtained in simulation with the classic models and the new model are compared. The values for the RMS with the other models evaluated are very high if they are compared to the low value obtained with the new model, and therefore it is not possible to discriminate this value in the scale. Figure 5 also shows the radical differences between the very low values for the responses obtained with the models studied and the high value obtained by the new model optimized. Both figures show definitely the extensive capability of the new model to simulate the evolution of an industrial fermentation process compared to the poor predictive capability of the other models.

Table 3. Optimized Parameters of New Model

kinetic parameter	optimized value
K_1	7.845e-005 h^{-1}
K_2	7.844e-04 $(g/L)^n$
n	3.631
μ_d	9.71e-02 h^{-1}
X_{vi}	0.104 g/L

The value obtained for X_{vi}, 0.104 g/L, is 30% over the initial total biomass measured, 0.35 g/L, a value not so far from 20%, the standard value used by Caro et al. (1996) and Macías et al. (1997), and it has been also used in this work with the simulations to test the other models. It should be considered that the value obtained was calculated without any limitation due to the initial total biomass, and thus the algorithm was free to explore higher or lower values of initial viability. The higher viability found in the optimization of the parameters compared to the value of Caro et al. (1996) and Macías et al. (1997) seems logical if one takes into account that the bacteria is able to adjust their life cycle to the industrial conditions.

In conclusion, it has been proved that the model proposed is capable of explaining the industrial process of acetic fermentation. Since it only depends on the ethanol concentration, it can simulate properly processes with different initial concentrations of ethanol and acetic

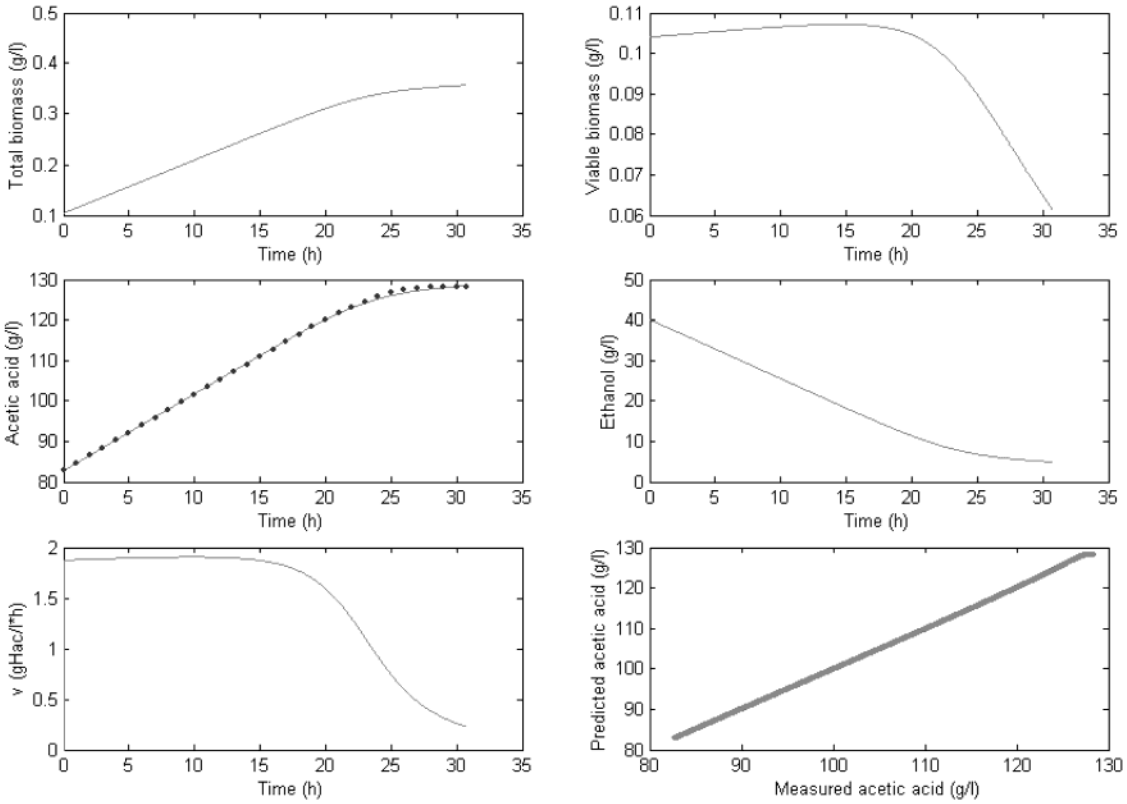

Figure 4. Simulation output of the new model with the optimized parameters.

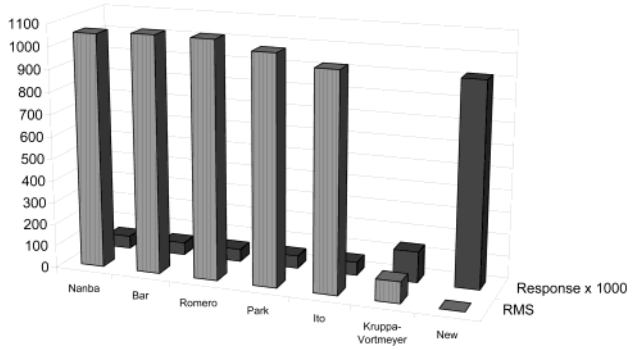

Figure 5. Comparison of values obtained in simulation for the RMS and the Response with all the models.

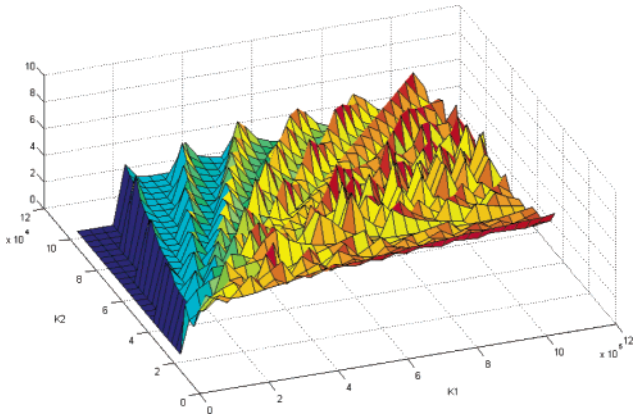

Figure 6. Response surface of the desirability function over K_1 and K_2. The rest of the parameters are maintained constant and equal to the optimized values of Table 3.

acid, whereas the temperature and aeration conditions are the same. Indeed, the model can be applied to different configurations of the reactors, with the same temperature and aeration conditions.

Response Surface Generated by the Desirability Function. In Figures 6 and 7 are drawn different projections of the desirability function over two of the parameters. In each graph, the other three parameters have been maintained constant and equal to the optimized values obtained by the algorithm, that have been reported in Table 3. The values for the desirability function have been obtained by simulations with the correspondent set of kinetic parameters and the same simulation environment applied in the genetic algorithm. The surfaces have been build with Matlab 6.1.0.450 (The MathWorks, Inc.), using the *surf* function.

Figure 6 shows the projection of the desirability function over a large range of values for K_1 and K_2. The surface is extremely badly behaved, with several local maximums. It is evident that gradient techniques and classical nongradient techniques as the Simplex or the Powell methods would have problems with this surface. Such nongradient techniques would find a local maximum that it would depend on the start point. On the other hand, an alternative to these methods is the performing of a grid search spanning the whole space of the parameters. However, because of the complexity of the surface, this method would have required a very thick grid to do the search along with guarantees of finding a good solution. Therefore, this method would become very time-consuming. The genetic algorithm method simplifies and improves this search. The advantages of using genetic algorithms applied to kinetic modeling have been reported in the Computational Methods section and the bad behavior of the response surface justifies further the applying of this technique.

Although the matrix of responses projected in this figure is very thick, the lowest values of the range are not represented enough, due to the extremely large range studied and the bad behavior of the response surface. The range of low values for K_1 and K_2 provides the simula-

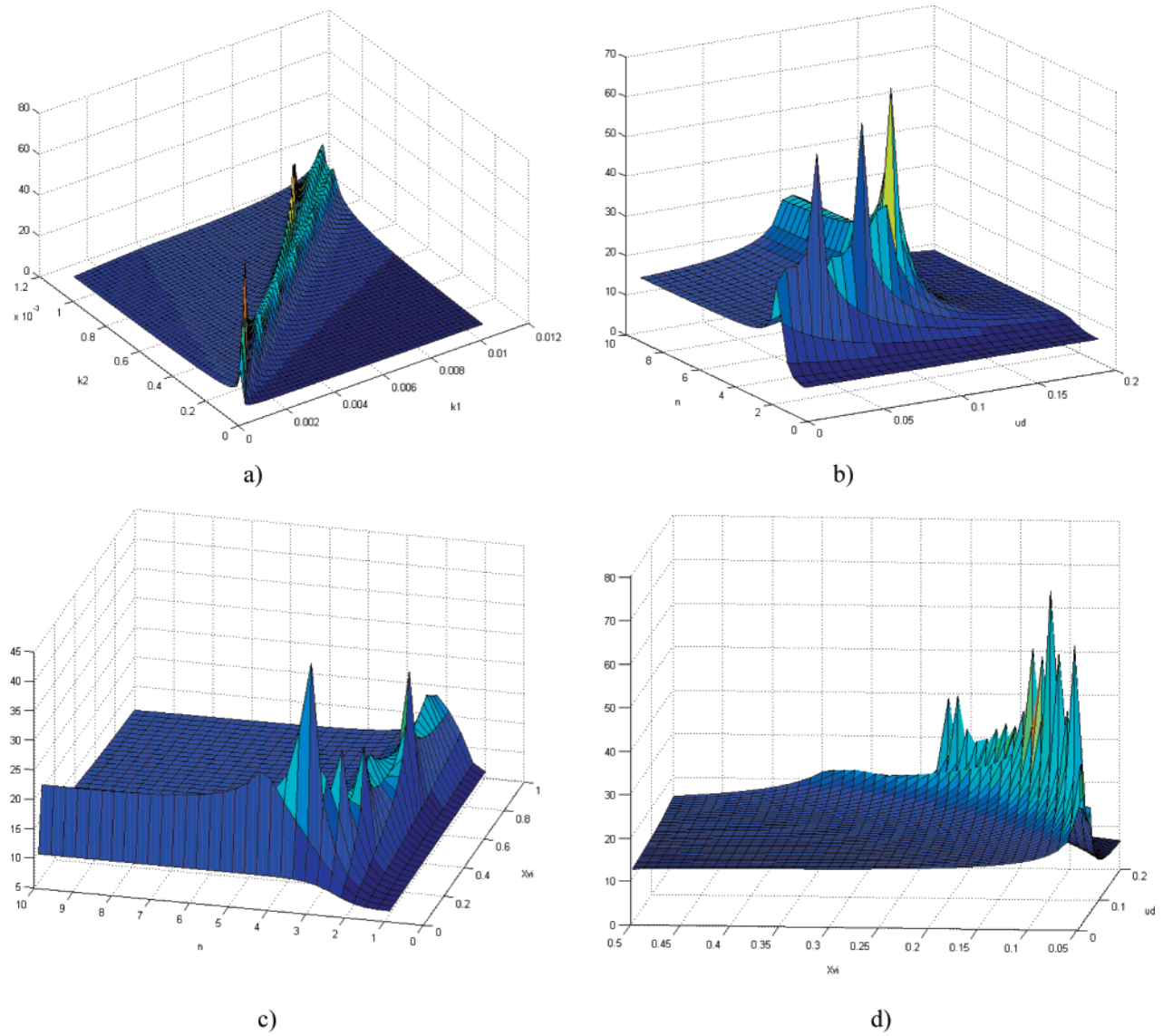

Figure 7. Response surface of the desirability function over (a) K_1 and K_2; (b) μ_d and n; (c) X_{vi} and n; (d) μ_d and X_{vi}. The rest of the parameters are maintained constant and equal to the optimized values of Table 3.

tions with the best values for the desirability function, so the values of the response in Figure 6 are low.

In Figure 7 are drawn four projections of values of the desirability function over four couples of kinetic parameters. The ranges are narrower than in Figure 6 and more closed to the final optimized values reported in Table 3. Therefore, the values for the desirability function are better than in Figure 6. In any way, the surfaces are very badly behaved, with several local maximums and the same conclusions that those inferred from Figure 6 can be applied to these figures. The global maximum found by the genetic algorithm is not shown in the graphs because of the amount of local maximums that can be found. Indeed, it would be necessary to obtain an extremely thick matrix of responses to show all the possible maximums that the function can reach. As has been explained before, it would be almost impossible to find the best set of parameters applying gradient search techniques, classic nongradient methods, or a full grid search.

Finally, an interesting conclusion about the values of K_1 and K_2 is inferred from Figure 6 and Figure 7a. The best results for the desirability function are obtained when K_1 and K_2 are very similar and they are within a low range of values, as has been reported before. In this way, in Figure 6 the surface adopts the form of chains of "mountains" that cross through the range. Each chain of maximums corresponds to similar values of K_1 and K_2 within a different range. Indeed, in Figure 7a is shown the chain of maximums that corresponds to similar values of K_1 and K_2 in a range closed to the optimized values.

Conclusions

The six models studied cannot explain the behavior of an industrial fermentation process. According to these models, the maximum acetic concentration that can be obtained is within the range of 83−100 g/L. These models propose some inhibitory effects of the acetic acid that cannot be inferred from an industrial point of view.

The new kinetic model proposed solves this problem, and the genetic algorithm can successfully optimize the kinetic parameters. Only a representative sequence of the acetic acid concentrations from the industrial fermentators is needed. The desirability function used as the evaluation function can select the best set of parameters for the model. The simulated acetic acid sequence ob-

tained with the model is perfectly adjusted to the representative sequence of industrial concentrations.

The projections of the desirability function over different couples of kinetic parameters show extremely complex and badly behaved surfaces, with several local maximums, making very difficult the search of the best set of parameters by classic gradient and nongradient techniques and by a full grid search.

Given the good results obtained with the model, it is currently being used to develop new industrial fermentation systems. Provided that the desirability function is adapted, the algorithm might be used to optimize the process in terms of economies.

Acknowledgment

The authors thank the Ministry of Agriculture and Food (INIA CAL01-053) and the Autonomous Government of La Rioja (Consejería de Educación, Juventud y Deportes under the research grant FPI-1999) for their financial support.

Notation

A	acetic acid concentration (g/L)
A_r	final acetic acid concentration reached in the real sequence (g/L)
A_s	final acetic acid concentration reached in the simulation (g/L)
B_r	slope of data with a linear behavior in the real sequence (0−20 h)
B_s	slope of data in the simulated sequence with a process time range of 0−20 hours
d_{cn}	value of the single desirability function for the y_{cn} response
D_n	value of the global desirability function for the n sample
DW	dry weight
E	ethanol concentration (g/L)
f_c	kind of single desirability function chosen for the selected criterion c
k	specific death rate for the conversion of viable cells into nonviable cells (h^{-1})
M_{EtOH}	molar mass of ethanol (g/mol)
M_{HAc}	molar mass of acetic acid (g/mol)
O	oxygen concentration (g/L)
q_A	specific rate of acetic acid production (h^{-1})
q_{Am}	maximum specific rate of acetic acid production (h^{-1})
r	observed cell growth rate (gDW/L·h)
r_A	overall acetic acid production rate (g/L·h)
r_{A-AcEt}	acetic acid consumption rate by ethyl acetate formation (g/L·h)
r_{A-X}	rate of acetic acid excreted by biomass (g/L·h)
r_d	overall cell death rate (gDW/L·h)
r_e	rate of consumption of organic cell matter in endogenous respiration (gDW/L·h)
r_E	overall rate of ethanol consumption (g/L·h)
r_{E-AcEt}	ethanol consumption rate by ethyl acetate formation (g/L·h)
r_{E-m}	ethanol consumption rate for the production of maintenance energy (g/L·h)
r_{E-P}	ethanol consumption rate for the formation of products (g/L·h)
r_{E-X}	ethanol consumption rate for the production of biomass (g/L·h)
r_g	overall cell growth rate (gDW/L·h)
r_l	cell lysis rate (gDW/L·h)
RMS	root-mean-square of the differences in the acetic acid concentrations between the simulated and the representative sequence
r_O	overall rate of oxygen consumption (g/L·h)
r_{O-m}	oxygen consumption rate for the production of maintenance energy (g/L·h)
r_{O-P}	oxygen consumption rate for the formation of products (g/L·h)
r_{O-X}	oxygen consumption rate for the production of biomass (g/L·h)
r_P	overall product formation rate (g/L·h)
r_S	overall rate of substrate consumption (g/L·h)
r_{S-m}	substrate consumption rate for the production of maintenance energy (g/L·h)
r_{S-P}	substrate consumption rate for the formation of products (g/L·h)
r_{S-X}	substrate consumption rate for the production of biomass (g/L·h)
t_r	process time in the real sequence (h)
t_s	process time in the simulation (h)
X_d	death biomass concentration (gDW/L)
X_{nv}	nonviable biomass concentration (gDW/L)
X_t	total biomass concentration (gDW/L)
X_v	viable biomass concentration (gDW/L)
X_{vi}	initial viable biomass concentration (gDW/L)
$Y_{A/E}$	acetic acid/ethanol stoichiometric coefficient
$Y_{A/O}$	acetic acid/oxygen stoichiometric coefficient
y_{cn}	response of the n sample for the c criterion
$Y_{E/O}$	ethanol/oxygen stoichiometric coefficient
$Y'_{X/E}$	biomass/ethanol yield factor
$Y'_{X/O}$	biomass/oxygen yield factor

Greek Symbols

μ	observed specific growth rate (h^{-1})
μ_d	overall specific death rate (h^{-1})
μ_g	overall specific growth rate (h^{-1})
μ_m	maximum specific growth rate (h^{-1})
γ	specific death rate for the conversion of nonviable cells into dead cells (h^{-1})

References and Notes

Bailey, J. E.; Ollis, D. F. *Biochemical Engineering Fundamentals*, 2nd ed.; McGraw-Hill International Editions: New York, 1986.

Bar, R.; Gainer, J. L.; Kirwan, D. J. An unusual pattern of product inhibition: Batch acetic acid fermentation. *Biotechnol. Bioeng.* **1987**, *29*, 796−798.

Berget, I.; Næs, T. Sorting of raw materials with focus on multiple end-product properties. *J. Chemom.* **2002**, *16*, 263−273.

Caro, I.; Macías, M.; Cantero, D. Optimum operating conditions in closed-system industrial acetifiers (batch operation): A study by computer simulation. *Chem. Eng. J.* **1996**, *62*, 183.

Cooney, C. L.; Petrides, D.; Barrera, M.; Evans, L. *Computer-Aided Design of a Biochemical Process*; ACS Symposium Series 39; American Chemical Society: Washington, DC, 1988; pp 39−61.

Cooney, M. J.; Goh, L. T.; Lee, P. L.; Johns, M. R. Structured model-based analysis and control of the hyaluronic acid fermentation by *Streptococcus zooepidemicus*: Physiological implications of glucose and complex-nitrogen-limited growth. *Biotechnol. Prog.* **1999**, *15*, 898−910.

Crundwell, F. K. Modelling, simulation, and optimisation of bacterial leaching reactors. *Biotechnol. Bioeng.* **2001**, *71*(4), 255−265.

Gómez, J. M.; Cantero, D. Kinetics of substrate consumption and product formation in closed acetic fermentation systems. *Bioprocess Eng.* **1998**, *18*, 439−444.

Harrington, E. C. The desirability function. *Ind. Qual. Control* **1965**, *21*, 494−498.

Hendriks, M. M. W. B.; de Boer, J. H.; Boey, P. Multicriteria decision making. *Chemom. Intell. Lab. Syst.* **1992**, *16*, 175−191.

Hodge, David B.; Karim, M. Nazmul. Modeling and advanced control of recombinant *Zymomonas mobilis* fed-batch fermentation. *Biotechnol. Prog.* **2002**, *18*, 572−579.

Huang, M. W.; Hsieh, C. C.; Arora, J. S. A genetic algorithm for sequencing type problems in engineering design. *Int. J. Numer. Methods Eng.* **1997**, *40*, 3105−3115.

Ito, T.; Sota, H.; Honda, H.; Shimizu, K.; Kobayashi, T. Efficient acetic acid production by repeated fed-batch fermentation using two fermentators. *Appl. Microbiol. Biotechnol.* **1991**, *36*, 295−299.

Keller, H. R.; Massart, D. L.; Brans, J. P. Multicriteria decision making: a case study. *Chemom. Intell. Lab. Syst.* **1991**, *11*, 175−189.

Kruppa, R. K.; Vortmeyer, D. Transient growth and product formation kinetics of acetic acid bacteria. *Bioprocess. Eng.* **1999**, *20*, 545−551.

Lucasius, C. B.; Kateman, G. Understanding and using genetic algorithms. Part 1. Concepts properties and context. *Chemom. Intell. Lab. Syst.* **1993**, *19*, 1−33.

Lucasius, C. B, Kateman, G. Understanding and using genetic algorithms. Part 2. Representation, configuration and hybridization. *Chemom. Intell. Lab. Syst.* **1994**, *25*, 99−145.

Macías, M.; Caro, I.; Cantero, D. Optimum operating conditions in closed-system industrial acetifiers (semi-continuous operation): a study by computer simulation. *Chem. Eng. J.* **1997**, *65* (3), 201−207.

Massart, D. L.; Vandeginste, B. G. M.; Buydens, L. M. C.; De Jong, S.; Lewi, P. J.; Smeyers-Verbeke, J. *Handbook of Chemometrics and Cualiametrics*, Part A; Elsevier: London, 1997.

Mesa, M.; Caro, I.; Cantero, D. Viability reduction of *Acetobacter aceti* due to the absence of oxygen in submerged cultures. *Biotechnol. Prog.* **1986**, *12*, 709−712.

Nanba, A.; Takumura, A.; Nagai, S. Synergistic effects of acetic acid and ethanol on the growth of *Acetobacter* sp. *J. Ferment. Technol.* **1984**, *6*(62), 501−505.

Ory, I.; Romero, L. E.; Cantero, D. Modelling the kinetics of growth of *Acetobacter aceti* in discontinuous culture: influence of the temperature of operation. *Appl. Microbiol. Biotechnol.* **1998**, *49*, 189−193.

Osborne, B. G.; Fearn, T.; Hindle, P. H. *Practical NIR Spectroscopy with Applications in Food and Beverage Analysis*, 2nd ed.; Longman Scientific & Technical: UK, 1993.

Park, Y. S.; Toda, K.; Fukaya, M.; Okumura, H.; Kawamura, Y. Production of a high concentration acetic acid by *Acetobacter aceti* using a repeated fed-batch culture with cell recycling. *Appl. Microbiol. Biotechnol.* **1991**, *35*, 149−153.

Perry, R. H.; Green, D. W. *Perry's Chemical Engineers' Handbook*, 7th ed.; McGraw-Hill Professional: New York, 1997.

Petrides, D. Biopro designer: an advanced computing environment for modelling and design of integrated biochemical processes. *Comput. Chem. Eng.* **1994**, *18*, 621−625.

Pinchuk, R. J.; Brown, W. A.; Hughes, S. M.; Cooper, D. G. Modelling of biological processes using self-cycling fermentation and genetic algorithms. *Biotechnol. Bioeng.* **2000**, *67*(1), 19−24.

Pizarro, Millán C.; Forina, M.; Casolino, M. C.; Leardi, R. Extraction of representative subsets by potential functions methods and genetic algorithms. *Chemom. Intell. Lab. Syst.* **1998**, *41*, 195−207.

Potocnik, P.; Grabec, I. Empirical modelling of antibiotic fermentation process using neural networks and genetic algorithms. *Math. Comput. Simul.* **1999**, *49*, 363−379.

Reijmers, T. H.; Wehrens, R.; Buydens, L. M. C. Quality criteria of genetic algorithms for construction of phylogenetic trees. *J. Comput. Chem.* **1999**, *20*, 867−876.

Romero, L. E.; Gómez, J. M.; Caro, I.; Cantero, D. A kinetic model for growth of Acetobacter aceti in submerged culture. *Chem. Eng. J.* **1994**, *54*, B15−B24.

Shimizu, H.; Yasuoka, K.; Uchiyama, K.; Shioya, S. Bioprocess fault detection by nonlinear multivariate analysis: Application of an artificial autoassociative neural networqk and wavelet filter bank. *Biotechnol. Prog.* **1998**, *14*, 79−87.

Sinclair, C. G.; Kristiansen, B. *Fermentation Kinetics and Modelling*, 1st ed.; Open University Press: London, 1987.

Sinclair, C. G.; Topiwala, H. H. Model for continuous culture which considers the viability concept. *Biotechnol. Bioeng.* **1970**, *12*, 1069−1070.

Wehrens, R.; Buydens, L. M. C. Evolutionary optimisation: a tutorial. *Trends Anal. Chem.* **1998**, *17*, 193−203.

Accepted for publication December 13, 2002.

BP0256871